

# Dynamical Precursors for Statistical Prediction of Stratospheric Sudden Warming Events

M. Jucker<sup>1\*</sup>, T. Reichler<sup>2</sup>

<sup>1</sup>School of Earth Sciences and ARC Centre of Excellence for Climate System Science, The University of Melbourne,  
Melbourne, Australia

<sup>2</sup>Department of Atmospheric Sciences, University of Utah, Salt Lake City, Utah

## Key Points:

- A statistical approach explores the sudden warming predictability beyond the ten-day limit of dynamical forecasts
- The approach utilizes upward wave activity and meridional potential vorticity gradient to determine conditional sudden warming probabilities
- The conditional probabilities show significant information gain over climatology out to one season

---

\*Current address: Climate Change Research Centre, University of New South Wales, Sydney, Australia

Corresponding author: Martin Jucker, [publications@martinjucker.com](mailto:publications@martinjucker.com)

**Abstract**

This work explores dynamical arguments for statistical prediction of Stratospheric Sudden Warming events (SSWs). Based on climate model output, it focuses on two predictors: upward wave activity in the lower stratosphere and meridional potential vorticity (PV) gradient in the upper stratosphere, and detects large values of these predictors. Then it quantifies how many SSWs are preceded by predictor events, and, inversely, how many events are followed by SSWs. This allows to compute conditional probabilities of future SSW occurrence. It is found that upward wave activity leads to important increases in SSW probability within the following three weeks, but is less important thereafter. A weak PV gradient is associated with increased SSW probability at short lags and, perhaps more importantly, decreased SSW probability at long lags. Finally, when both predictors are considered in combination, the information gain is large on the weekly and small but significant on the intra-seasonal time scale.

**1 Introduction**

Stratospheric Sudden Warming Events (SSWs) have been a focus of research on stratosphere-troposphere coupling for a while now. Eliassen-Palm (EP) fluxes of planetary scale can propagate from the troposphere into the stratosphere in northern hemisphere winter, when mid- to high-latitude zonal winds are westerly throughout the stratosphere (and not too strong) [Charney and Drazin, 1961; Dickinson, 1969]. Breaking of those waves and the associated EP flux divergence can lead to the breakdown of the stratospheric polar vortex [Matsuno, 1971; Holton, 1974; McIntyre, 1982], causing SSWs which in turn can influence the state of the troposphere on the seasonal time scale [e.g. Baldwin and Dunkerton, 2001; Sigmond et al., 2013; Shaw et al., 2014; Scaife et al., 2017]. Thus, enhanced upward EP fluxes play an important role in the evolution of sudden warmings [e.g. Matsuno, 1971; Limpasuvan et al., 2004; Polvani and Waugh, 2004; Nishii et al., 2009; Ayrarzagüena et al., 2011; Schneidereit et al., 2017], and peak about a week before the onset date [Garfinkel et al., 2010; Jucker, 2016; Dunn-Sigouin and Shaw, 2015; Martineau and Son, 2015; Charlton and Polvani, 2007; Nakagawa and Yamazaki, 2006].

However, various authors also note that enhanced EP flux might not be as important as previously thought. Although probably *necessary* (see below), it may not provide a *sufficient* condition for the occurrence of a sudden warming [Scott and Polvani, 2004, 2006; Matthewman and Esler, 2011; Esler and Matthewman, 2011; Albers and Birner, 2014; Jucker, 2016; Birner and Albers, 2017]. Indeed, while easterly zonal momentum is required to reverse the polar vortex, its deposition also has to be at the right place. Following linear wave propagation theory, EP fluxes are directed towards higher refractive index [Palmer, 1981; Karoly and Hoskins, 1982]. The only term within the refractive index depending on the dynamical background state of the atmosphere is proportional to the meridional potential vorticity gradient (henceforth "PV gradient")  $q_\phi$  [Matsuno, 1970]. The PV gradient is proportional to second derivatives of zonal wind (Eq. (1)) and therefore sensitive to small wind perturbations. As a result, even weak forcing can change the refractive index substantially and hence may alter the wave propagation and divergence [Butchart et al., 1982]. Previous work [e.g. Albers and Birner, 2014; Jucker, 2016] has shown that the PV gradient sharpens along the vortex edge long before anomalous upward EP flux peaks, also known as "preconditioning" [Labitzke, 1977, 1981; Schoeberl, 1978; McIntyre, 1982; Bancalá et al., 2012]. The long lead time between the vortex sharpening and the onset of sudden warmings suggests that the stratospheric PV gradient could be a useful predictor for SSWs.

Therefore, this work will study the potential for improved statistical prediction of SSWs based on the pre-SSW evolution of EP flux and PV gradient, the two main quantities determining when, how much and where in the stratosphere easterly momentum is deposited. We will make use of general circulation model (GCM) data for meaningful statistical analyses, as observational and/or reanalysis data contains too few SSWs.

In section 2, we describe the GCM setup and derived variables to be used for the study. Section 3 validates the model and quantifies the relationship between precursors and SSWs. Section 4 examines the conditional SSW probabilities before concluding remarks in section 5.

## 2 Data and methods

We use a nearly 10,000 year long control integration with a stratosphere-resolving version of the CM2.1 model from GFDL, described in *Horan and Reichler* [2017]. These authors showed that the stratospheric dynamics of this model compare well to reanalysis in terms of SSW frequency, seasonal evolution of the polar vortex strength and its variability. Multiple lines of work have also shown that CM2.1 simulates a very reasonable tropospheric climate [e.g. *Reichler and Kim*, 2008]. We apply the *Charlton and Polvani* [2007] definition of major SSWs. Explicitly, we require a reversal of the zonally averaged zonal wind at 60°N and 10 hPa, with a return to westerly winds for at least 10 consecutive days during the same season. Also, two zero crossings have to be separated by at least 20 days to be counted as distinct events.

We detect SSWs from December to March, leading to a mean frequency of 5.9 SSWs per decade, in accordance with most other studies [*Palmeiro et al.*, 2015; *Butler et al.*, 2015; *Charlton et al.*, 2007]. We are not including November as we consider conditions up to 90 days before any particular SSW, and want to minimize the number of summer days included in our analysis.

We compute the meridional gradient of potential vorticity [*Matsuno*, 1970] in the form given by *Simpson et al.* [2009],

$$q_\phi = \int_{\phi_0}^{\phi_1} d\phi \left\{ 2\Omega \cos \phi - \left[ \frac{(\bar{u} \cos \phi)_\phi}{a \cos \phi} \right] + \frac{af^2}{R_d} \left( \frac{p\theta}{T} \frac{\bar{u}_p}{\theta_p} \right)_p \right\} \bigg/ \int_{\phi_0}^{\phi_1} \cos \phi d\phi, \quad (1)$$

where standard notation is used. Overbar ( $\bar{\cdot}$ ) denotes zonal mean and subscripts represent derivatives. We compute the meridional mean value between  $\phi_0 = 55^\circ\text{N}$  and  $\phi_1 = 75^\circ\text{N}$  and at 30 hPa, as this is where the signal in  $q_\phi$  is strongest.

The vertical component of the quasi-geostrophic Eliassen-Palm flux [*Eliassen and Palm*, 1961] is calculated following *Andrews et al.* [1987]

$$F_p = a \cos \phi f \frac{\overline{v'\theta'}}{\theta_p}, \quad (2)$$

where primes denote zonal asymmetries. We will only be interested in the hemispherically averaged EP fluxes at 100 hPa, defined as

$$F_z = - \int_{\phi_2}^{\phi_3} F_p d\phi \bigg/ \int_{\phi_2}^{\phi_3} \cos \phi d\phi, \quad (3)$$

where the average goes from from  $\phi_2 = 20^\circ\text{N}$  to  $\phi_3 = 90^\circ\text{N}$  and the minus sign was added to ensure that positive  $F_z$  means upward propagation. We standardize both variables relative to the day of the year by first removing the daily climatological mean and then dividing by the daily standard deviation.

We define an event  $E$  as the crossing of a given threshold of one or more variables. Any consecutive days where the variables are beyond the threshold are considered to be part of the same event.

Then, the conditional probabilities are computed by counting the number of relevant events in the model simulations:

$$P(SSW|E)(l) = \frac{\# \text{ events } E \text{ at lag } l \text{ of a SSW}}{\# \text{ of events } E}, \quad (4)$$

The climatological event and SSW probabilities are

$$\overline{P(X)} = \frac{\# X \text{ in data}}{(\# \text{ days in extended winter period}) \cdot (\# \text{ years})}, \quad (5)$$

where  $X$  is any event, including SSWs. The empirically derived climatological SSW probability is  $P(SSW) = 0.49\%$ .

We will compare the conditional probabilities (4) to the climatological probability  $\overline{P(SSW)}$  (5) to estimate the impact of event  $E$  onto the probability of SSW occurrence. We note that by comparing  $P(SSW|E)$  to  $\overline{P(SSW)}$  we assume for the latter that all days are independent and have the same (climatological) probability of SSW occurrence. Of course, this is an approximation, as e.g. the probability of occurrence of an SSW is zero directly after an SSW, violating the assumption of independence. However, we will show a posteriori that the approximation is reasonable, as  $P(SSW|E)$  converges towards  $\overline{P(SSW)}$  at long lags. We expect that any event  $E$  becomes independent from SSWs at sufficiently large lags  $n$ , i.e.  $P(SSW|E) \xrightarrow{n \gg 1} P(SSW)$ , and we verify in Fig. 3 that  $P(SSW) \approx \overline{P(SSW)}$  which validates our approximation.

In addition, we compute the fraction of SSWs preceded by event  $E$  within  $n$  days (Fig. 2), and compare this to the empirical probability of event  $E$  during the same  $n$  days. Keeping with the above notation of  $X$  as a placeholder for either SSW or event  $E$ , we compute the probability of one or more events  $X$  happening within  $n$  days (irrespective of any other event or SSW occurring within the same time period) as

$$\mathcal{P}(X)(n) = 1 - \prod_{i=1}^n \left(1 - \overline{P(X)}(i)\right). \quad (6)$$

### 3 SSW precursors

As described in the introduction, both the *strength* and the *location* of EP wave breaking is important. For planetary Rossby waves, the meridional potential vorticity gradient represents the dynamical part of the refractive index [Albers and Birner, 2014]. Therefore, we consider here the upward EP flux in the lower stratosphere (100 hPa) as the source for dynamical perturbations, and the stratospheric meridional PV gradient (at 30 hPa) as the determining quantity for the propagation (and breaking) of those perturbations.

In order to verify that our experiments reproduce previous findings, we composite the evolution of  $F_z$  and  $q_\phi$  in anomalous and standardized form in Fig. 1. The upward wave activity does not significantly deviate from its climatological distribution (both mean and standard deviation) more than about three weeks before onset (transparent shading in Fig. 1a), but strongly peaks during the week before the onset. The PDFs in Fig. 1b) neatly show how the distribution just before the onset is distinct from the PDF including all days.

Fig. 1c) shows that the composite PV gradient is positive from about 10-70 days prior to onset, and the PDFs in panel d) are also different between pre-SSW days and all simulation days. Evidently, the signal is weaker for  $q_\phi$  than for  $F_z$ , but in contrast to the latter, the composite evolution of  $q_\phi$  differs significantly from the climatological distribution for lags of 90 days and more: although the mean returns to zero, the 5<sup>th</sup> percentile remains significantly below the climatological 5<sup>th</sup> percentile.

Rather than relying on composites and mean evolution, we next quantify the fraction of SSWs which are preceded by anomalous upward EP flux and meridional PV gradient. We define the 5<sup>th</sup> and 95<sup>th</sup> percentiles as event thresholds, which are  $-1.77\sigma$  and  $1.47\sigma$  for  $F_z$  and  $-1.67\sigma$  and  $1.60\sigma$  for  $q_\phi$ .

The left column of Fig. 2 shows the fraction of SSWs in the dataset which are preceded by at least one event (thick lines) as a function of lag before onset. Lag increases from right

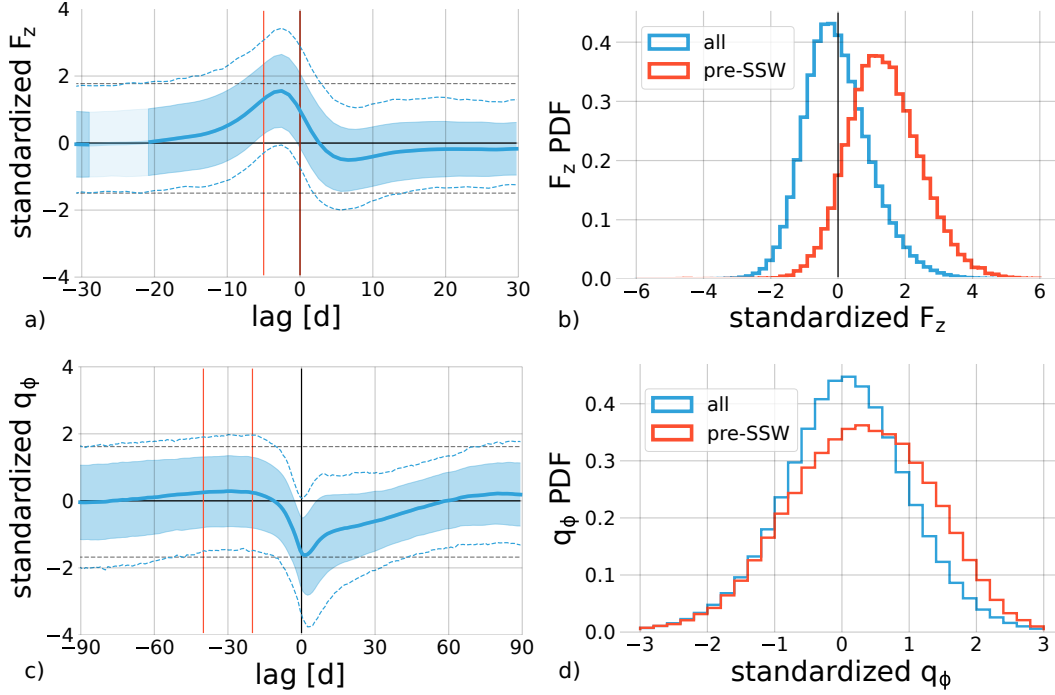


**Figure 1.** (left) SSW composites (onset at lag 0) of a) upward EP flux at 100 hPa, and c) meridional potential vorticity gradient at 30 hPa. The blue shading shows the range of one standard deviation around the mean, and is transparent where the composite does not differ significantly in both mean and standard deviation from the entire time series (10,000 member bootstrap plus Kolmogorov-Smirnov test). The dashed blue lines show the 5th and 95th percentiles of the composites, whereas the horizontal dashed gray lines show the 5th and 95th percentiles of the entire dataset. (right) Histograms of the same quantities, for all days (blue) and days associated with SSWs at lags denoted by the vertical red lines in the left panels (red).

to left. The fractions are compared to the values we would expect if the events and SSWs were independent, and are estimated from climatology using Eqs. (5) and (6). The shaded area is the difference between the independent and the observed values.

The right column of Fig. 2 shows the slopes of the SSW fractions shown on the left to demonstrate at which lags most of the increase/decrease happens. We emphasize that an ‘event’ here means the first crossing of a given threshold: If, for instance, the upward EP flux goes beyond the 95<sup>th</sup> percentile five days prior to onset and remains above the threshold until onset, the corresponding event of  $F_z > 95^{\text{th}}$  will only be triggered at lag -5, and no event is detected at shorter lags. Similarly, on any given day,  $P(F_z > 0)$  will be much lower than 50%. This is why e.g. the thick blue line of observed SSW fraction in Fig. 2a) is below the thin line at short lags, and the thin blue line based on the climatological occurrence of  $F_z$  events in Fig. 2b) does not start at 50% but at 7.5%, even though about 50% of all individual days have  $F_z > 0$ . Fig. 2b) shows that  $F_z > 0$  events have a higher probability of occurrence than if they were independent of SSWs between about lags -18 and -4, with a peak around one week before onset (thick blue line). At short lags, the fraction of SSWs preceded by an  $F_z > 0$  event is lower than if  $F_z$  and SSWs were independent (Fig. 2a), blue line), but becomes larger around lag -9 when going towards higher negative lags (towards the left), and remains higher at longer negative lags. Higher threshold events of  $F_z > 95^{\text{th}}$  percentile happen more often than if they were independent of SSWs from about lag -11 all the way to onset, with a peak around lag -3 (Fig. 2b), red line). Both the red and blue lines are below the independent (climatological) thin lines at higher lags. The resulting fraction of SSWs as-

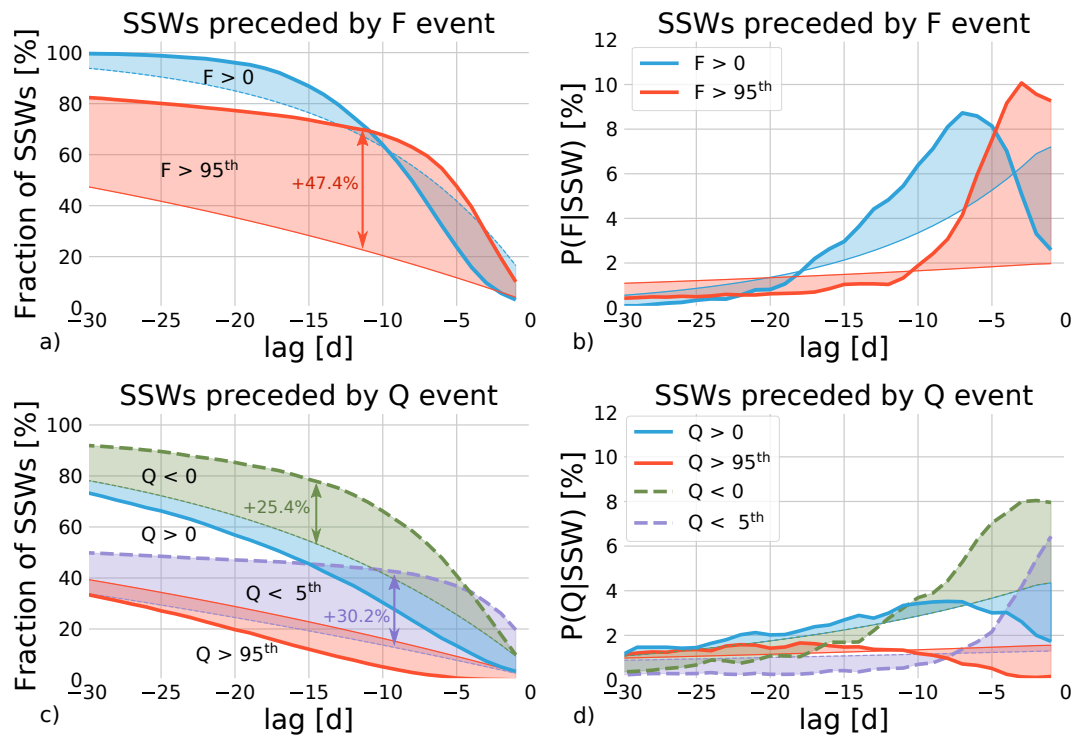


**Figure 2.** (top left) Cumulative fraction of SSWs which are preceded by a  $F_z > 0$  (blue) or  $F_z > 95^{\text{th}}$  percentile event (red), as a function of lag before onset (which increases from right to left). (top right) Daily probability of event occurrence prior to onset, which is the slope of the cumulative fraction. (bottom) Same but for  $q_\phi \leq 0$ ,  $q_\phi < 5^{\text{th}}$  and  $q_\phi > 95^{\text{th}}$  percentiles. The thin lines are computed from Eq. (6).

sociated with such an event is always considerably higher than the same quantity assuming independence (red shaded area in Fig. 2a), with a maximum difference of 47.4% around lag -12. This is because upward EP flux starts to strengthen about two to three weeks prior to onset, and becomes steadily stronger as we move closer to the SSW, which means it will trigger a  $F_z > 0$  event first and a  $F_z > 95^{\text{th}}$  percentile event closer to onset, just like depicted in Fig. 2b).

Looking at the bottom panels of Fig. 2, the evolution of anomalously negative  $q_\phi$  is similar to  $F_z > 0$ , with  $q_\phi < 0$  events becoming more numerous than expected from independence at about lag -13 and  $q_\phi < 5^{\text{th}}$  percentile events doing the same around lag -8 (green and purple dashed lines in Fig. 2d). For positive  $q_\phi$  events, the evolution is mirrored: The fraction of SSWs for both  $q_\phi > 0$  and  $q_\phi > 95^{\text{th}}$  percentile is lower than climatology (i.e. assuming independence of  $q_\phi$ ) at short lags (Fig. 2c), blue and red), and the daily event probabilities change from lower to higher than expected from climatology with increasing lag before onset (Fig. 2d), blue and red). Both curves remain above the daily probabilities estimated from climatology at long lags. The fraction of SSWs with negative PV gradient events is much larger than the climatological estimates (Fig. 2c, green and purple), with maximum differences of 25.4% at lag -14 and 30.2% at lag -9 respectively.

The positive PV gradient events are associated with a slightly smaller SSW fraction at short lags, which converges back to the climatological value at longer lags, and eventually becomes slightly higher at very long lags (not shown). Particularly from the daily event probabilities, we conclude that positive  $q_\phi$  events, and therefore steeper meridional PV gradients, are associated with future SSWs at large lags, and that weaker meridional PV gradients are associated with future SSWs at lags shorter than two weeks.

#### 4 Conditional SSW probabilities

We now use the results from the previous section to construct predictors for SSWs. That is, we invert the usual compositing or life cycle approach and detect instead single  $F_z$  and  $q_\phi$  events. Then, we compute the probability of an SSW in the future, given an  $F_z$  or  $q_\phi$  event happened (conditional probability). We will concentrate on the  $5^{\text{th}}$  and  $95^{\text{th}}$  percentile thresholds, and from now on refer to them as ‘negative’ and ‘positive’ thresholds.

The important quantity to compute is the conditional probability  $P(SSW|E)$ , i.e. the probability of a future SSW, given that a predefined event  $E$  has been detected. To investigate the potential for seasonal prediction we will consider a future time range of up to 90 days. Fig. 3 shows  $P(SSW|E)$  for different events  $E$ , normalized to  $\overline{P(SSW)}$ . Note that all values converge toward unity at long lags, which means that  $P(SSW|E) \rightarrow \overline{P(SSW)}$ . It is also clear that at long lags events  $E$  and SSWs must be independent, meaning that  $\overline{P(SSW|E)} \rightarrow \overline{P(SSW)}$ . Therefore, the empirically determined probability  $\overline{P(SSW)}$  equals  $\overline{P(SSW)}$  as defined by Eq. (5), which validates our approach to compare against  $\overline{P(SSW)}$  as outlined in the introduction.

##### 4.1 Upward Eliassen-Palm fluxes

Fig. 3a) shows  $P(SSW|F)$  as a function of lag, that is, the probability of detecting an SSW  $x$  days in the future (lag  $> 0$ ), given that we have detected a  $F$  event today (lag 0). The daily probability (i.e., the probability of occurrence at each individual lag) is given by Fig. 3d). The red (blue) line shows the probabilities for the positive (negative) threshold, and the black line the climatological value  $\overline{P(SSW)}$ .

There is a large gain in information after the occurrence of a strong upward EP flux event (Fig. 3a), red line), with the biggest increase in SSW probability (factor of 5) during the first week after the event.  $P(SSW|F)$  is significantly larger than  $\overline{P(SSW)}$  for just over two weeks, and there is a slightly (but statistically significant) lower SSW probability from about

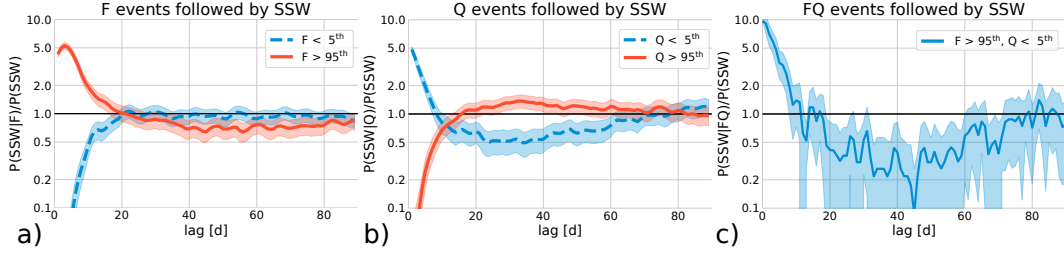


**Figure 3.** Conditional SSW probabilities, normalized to climatological SSW probability  $\overline{P(SSW)} = 0.49\%$ . a)  $P(SSW|F)$ , i.e. SSW probability given large positive (negative)  $F_z$  anomaly at lag 0 in red (blue). b)  $P(SSW|Q)$ , i.e. SSW probability given large positive (negative)  $q_\phi$  anomaly at lag 0 in red (blue). c)  $P(SSW|FQ)$ , i.e. SSW probability given large positive  $F_z$  anomaly at lag 0 concurrent with large positive (negative)  $q_z$  anomaly in red (blue). All conditional probabilities converge towards  $\overline{P(SSW)}$  (unity in the plots). Colored shading shows  $\pm 2\sigma$  from the mean obtained from a 10,000-member bootstrap estimate.

five weeks onwards. About 20% of all positive  $F_z$  events are followed by an SSW within two weeks (computed using Eq. (6), not shown). For the negative  $F_z$  threshold (blue dashed line in Fig. 1a),  $P(SSW|F)$  is more than an order of magnitude smaller than  $\overline{P(SSW)}$  for about a week, and converges toward  $\overline{P(SSW)}$  around the same time that the positive threshold does (around 20 days). Only 2% of all negative  $F_z$  events are followed by an SSW within two weeks (not shown). In contrast to the positive threshold, the negative threshold in  $F_z$  has no influence on SSW probability for lags beyond three weeks. To summarize, the power of prediction of  $F_z$  is greatest during the first week, decreases rapidly up to about 20 days, and it does not contribute to increased prediction skill beyond four weeks.

#### 4.2 Potential vorticity gradient

Similar to a negative  $F_z$  event, the SSW probability decreases by an order of magnitude within the first week after a positive PV gradient event (Fig. 3b, red line), and crosses the  $\overline{P(SSW)}$  mark around two weeks after the event. Then,  $P(SSW|Q)$  becomes slightly larger than  $\overline{P(SSW)}$  between four and five weeks after the event.

Negative PV gradients (blue dashed) are similar in effect to positive  $F_z$  at short lags, as they increase the immediate SSW probability up to five-fold within the first week. However, in contrast to  $F_z$ , the SSW probabilities are lower than  $\overline{P(SSW)}$  starting from the second week up to about two months. Three to five weeks after a negative  $q_\phi$  event, the SSW probability is halved compared to  $\overline{P(SSW)}$ . Beyond two months,  $P(SSW|Q)$  converges back to  $\overline{P(SSW)}$ . About 12% (3%) of all negative (positive)  $q_\phi$  events are followed by an SSW within two weeks (not shown).

Thus, to summarize our results so far: For the short term, the use of  $F_z$  as a predictor for an SSW occurrence is powerful, but yields little useful information beyond three weeks. Depending on the sign of the  $q_\phi$  threshold, the meridional PV gradient is just as good a predictor as  $F_z$  in the short term. But it adds significant information at long lags, as e.g.  $P(SSW|Q)$  is statistically significantly lower (up to a factor of two) than  $\overline{P(SSW)}$  15-60 days into the future.

#### 4.3 Combined probabilities

Following the dynamical idea that the PV gradient influences the orientation of EP fluxes, and that the PV gradient can therefore make the same EP flux more or less “efficient” in driving SSWs, we now consider the union of both events. That is, we compute

$P(SSW|F \cap Q)$ , the probability of a SSW happening within a certain time lag after upward EP flux crosses a specified threshold ( $F$  event) and the meridional PV gradient is larger (weaker) than a given positive (negative) threshold ( $Q$  event) (Fig. 3c).

There are now four possible combinations between the thresholds used in Figs. 3a) and b). However, as the negative  $F_z$  threshold corresponds to strongly decreased EP flux, there is no wave activity to be re-directed by the PV gradient. Also, the positive  $F_z$  and  $q_\phi$  events have opposing effects on the SSW probability (Figs. 3a and b). Therefore, we only show the probabilities for the combination of the positive  $F_z$  and the negative  $q_\phi$  thresholds in Fig. 3c).

At short lags ( $\sim$ first week), the combination of the two precursors about doubles the SSW probability compared to each precursor individually, and it is now a full order of magnitude larger than the climatological value. Computing the cumulative probabilities for the first week (7 days, Eq. (6)), we get a  $\sim 6x$  higher probability of any SSW happening within that period if we use the precursors (19% vs. 3.3%, not shown).

At long lags ( $\sim 20-60$  days),  $P(SSW|F \cap Q)$  is 2-5 times smaller than climatology. In other words, the occurrence of SSWs is strongly reduced 20-60 days after a  $F \cap Q$  event. In general,  $P(SSW|F \cap Q)$  follows the  $P(SSW|Q < 0)$  case (blue dashed line in Fig. 3b), but the increase and decrease in SSW probability is more pronounced. The (cumulative) probability of an SSW occurring within this time period is about 3x lower (6.2% vs. 17.3%, not shown) if we use the information from the precursors.

## 5 Conclusions

This study quantifies the probability of Stratospheric Sudden Warming event (SSW) occurrence as a function of two dynamical precursors. Based on earlier theoretical work, we define the precursor events as the crossing of thresholds of a) anomalous upward Eliassen-Palm flux at 100 hPa ( $F_z$ ) and b) anomalous stratospheric meridional potential vorticity (PV) gradient at 30 hPa ( $q_\phi$ ). Then, we show how the future occurrence of SSWs is statistically impacted by these events.

We find that  $F_z$  yields additional information for lead times of up to three weeks, whereas  $q_\phi$  impacts the probability of SSW occurrence for both short and long lead times: Anomalously weak PV gradients favor SSW occurrence for about one week, and make them less probable from one week to two months ahead. Anomalously strong PV gradients predict very low SSW probabilities for about two weeks, but slightly increased SSW probability for all longer lead times, including the seasonal time scale.

Combining  $F_z$  and  $q_\phi$  amplifies both the short and long term SSW probability signal. For instance, the probability of an SSW occurring the day after  $F_z$  crosses the 95<sup>th</sup> percentile ( $1.75\sigma$ ) while  $q_\phi$  is below the 5<sup>th</sup> percentile ( $-1.67\sigma$ ) is an order of magnitude higher than the probability based on climatology (Fig. 3c). This translates into a 19% chance of an SSW occurring within the first 7 days, compared to 3.3% within the same time period if we do not use the two precursors (as computed using Eq. (6)). It is interesting to note that the  $\sim 10$  day window of increased SSW probability is similar to the current limit of dynamical forecasting models to predict SSWs [Tripathi *et al.*, 2015, 2016; Karpechko, 2018]. However, and perhaps more importantly, our method can also give useful guidance on much longer time scales: The SSW probability is significantly reduced compared to the independent estimate from climatology 20-60 days after the above events are detected. Whereas the independent estimate is  $\sim 17\%$  for this time period, it is reduced to 6% when using the information from the precursors. Finally, we note that the above cited numbers depend on the exact threshold choices, lead times, and are also reported as seasonal averages: Any different combination of these parameters would yield different numbers, but the overall conclusions would remain the same. We emphasize that this study is the first to attempt statistical SSW prediction based on dynamical arguments. We also note that one could explore other predictors or combina-

tions thereof, but this is subject to a more comprehensive study which we leave for future work.

### Acknowledgments

TR acknowledges support from NSF grant 1446292. MJ acknowledges support from the Australian Research Council (ARC) Centre of Excellence for Climate System Science (CE110001028), and ARC grant FL150100035 during the revision of this manuscript. This work used the `xarray` [Hoyer and Hamman, 2017], `parmap` [https://github.com/zeehio/parmap], and `aostools` [Jucker, 2018] packages. We thank Eve Slavich from UNSW Stats Central for statistical support. We also acknowledge the Center for High Performance Computing at the University of Utah and the National Computational Infrastructure in Canberra for providing compute infrastructure and computing time. Derived datasets and the analysis script are published [Jucker and Reichler, 2018], and the full GCM data is available upon request with the authors.

### References

- Albers, J. R., and T. Birner (2014), Vortex Preconditioning due to Planetary and Gravity Waves prior to Sudden Stratospheric Warmings, *Journal of the Atmospheric Sciences*, 71(11), 4028–4054, doi:10.1175/JAS-D-14-0026.1.
- Andrews, D. G., J. R. Holton, and C. B. Leovy (1987), *Middle Atmosphere Dynamics*, International geophysics series, Academic Press.
- Ayarzagüena, B., U. Langematz, and E. Serrano (2011), Tropospheric forcing of the stratosphere: A comparative study of the two different major stratospheric warmings in 2009 and 2010, *Journal of Geophysical Research*, 116(D18), D18,114, doi: 10.1029/2010JD015023.
- Baldwin, M. P., and T. J. Dunkerton (2001), Stratospheric harbingers of anomalous weather regimes., *Science (New York, N.Y.)*, 294(5542), 581–4, doi:10.1126/science.1063315.
- Bancalá, S., K. Krüger, and M. Giorgetta (2012), The preconditioning of major sudden stratospheric warmings, *Journal of Geophysical Research Atmospheres*, 117(4), 1–12, doi:10.1029/2011JD016769.
- Birner, T., and J. R. Albers (2017), Sudden Stratospheric Warmings and Anomalous Upward Wave Activity Flux, *Sola*, 13A(Special\_Edition), 8–12, doi:10.2151/sola.13A-002.
- Butchart, N., S. A. Clough, T. N. Palmer, and P. J. Trevelyan (1982), Simulations of an observed stratospheric warming with quasigeostrophic refractive index as a model diagnostic, *Quarterly Journal of the Royal Meteorological Society*, 108(457), 475–502, doi: 10.1002/qj.49710845702.
- Butler, A. H., D. J. Seidel, S. C. Hardiman, N. Butchart, T. Birner, and A. Match (2015), Defining sudden stratospheric warmings, *Bulletin of the American Meteorological Society*, 96(2), 150904101253,006, doi:10.1175/BAMS-D-13-00173.1.
- Charlton, A. J., and L. M. Polvani (2007), A New Look at Stratospheric Sudden Warmings. Part I: Climatology and Modeling Benchmarks, *Journal of Climate*, 20(3), 449–469, doi: 10.1175/JCLI3996.1.
- Charlton, A. J., L. M. Polvani, J. Perlwitz, F. Sassi, E. Manzini, K. Shibata, S. Pawson, J. E. Nielsen, and D. Rind (2007), A New Look at Stratospheric Sudden Warmings. Part II: Evaluation of Numerical Model Simulations, *Journal of Climate*, 20(3), 470–488, doi: 10.1175/JCLI3994.1.
- Charney, J., and P. Drazin (1961), Propagation of Planetary-Scale Disturbances from the Lower into the Upper Atmosphere, *J. Geophys. Res.*, 66, 83–109.
- Dickinson, R. E. (1969), Vertical Propagation of Planetary Rossby Waves through an Atmosphere with Newtonian Cooling, *Journal of Geophysical Research*, 74(4), 929–938.
- Dunn-Sigouin, E., and T. A. Shaw (2015), Comparing and contrasting extreme stratospheric events, including their coupling to the tropospheric circulation, *Journal of Geophysical*

- Research: Atmospheres*, 120(4), 1374–1390, doi:10.1002/2014JD022116.
- Eliassen, A., and T. Palm (1961), On the transfer of energy in stationary mountain waves, *Geophys. Publ.*, 22(3), 1–23.
- Esler, J. G., and N. J. Matthewman (2011), Stratospheric Sudden Warmings as Self-Tuning Resonances. Part II: Vortex Displacement Events, *Journal of the Atmospheric Sciences*, 68, 2505–2523, doi:10.1175/JAS-D-11-08.1.
- Garfinkel, C. I., D. L. Hartmann, and F. Sassi (2010), Tropospheric precursors of anomalous northern hemisphere stratospheric polar vortices, *Journal of Climate*, 23(12), 3282–3299, doi:10.1175/2010JCLI3010.1.
- Holton, J. R. (1974), Forcing of Mean Flows by Stationary Waves, *Journal of the Atmospheric Sciences*, 31(4), 942–945, doi:10.1175/1520-0469(1974)031<0942:FOMFBS>2.0.CO;2.
- Horan, M. F., and T. Reichler (2017), Modeling Seasonal Sudden Stratospheric Warming Climatology Based on Polar Vortex Statistics, *Journal of Climate*, 30(24), 10,101–10,116, doi:10.1175/JCLI-D-17-0257.1.
- Hoyer, S., and J. J. Hamman (2017), xarray: N-D labeled Arrays and Datasets in Python, *Journal of Open Research Software*, 5, 1–6, doi:10.5334/jors.148.
- Jucker, M. (2016), Are Sudden Stratospheric Warmings Generic? Insights from an Idealized GCM, *Journal of the Atmospheric Sciences*, 73(12), 5061–5080, doi:10.1175/JAS-D-15-0353.1.
- Jucker, M. (2018), mjucker/aostools: aostools v2.1.5, doi:10.5281/ZENODO.1252733.
- Jucker, M., and T. Reichler (2018), Analysis for "Dynamical Precursors for Statistical Prediction of Stratospheric Sudden Warming Events", doi:10.17632/ffhv8kn7m5.2.
- Karoly, D. J., and B. J. Hoskins (1982), Three Dimensional Propagation of Planetary Waves, *Journal of the Meteorological Society of Japan. Ser. II*, 60(1), 109–123, doi: 10.2151/jmsj1965.60.1\_109.
- Karpechko, A. Y. (2018), Predictability of Sudden Stratospheric Warmings in the ECMWF extended range forecast system, *Monthly Weather Review*, pp. 17–0317, doi: 10.1175/MWR-D-17-0317.1.
- Labitzke, K. (1977), Interannual Variability of the Winter Stratosphere in the Northern Hemisphere, doi:10.1175/1520-0493(1977)105<0762:IVOTWS>2.0.CO;2.
- Labitzke, K. (1981), Stratospheric-mesospheric midwinter disturbances: A summary of observed characteristics, *Journal of Geophysical Research*, 86(C10), 9665, doi: 10.1029/JC086iC10p09665.
- Limpasuvan, V., D. W. J. Thompson, and D. L. Hartmann (2004), The Life Cycle of the Northern Hemisphere Sudden Stratospheric Warmings, *Journal of Climate*, 17(13), 2584–2596, doi:10.1175/1520-0442(2004)017<2584:TLCOTN>2.0.CO;2.
- Martineau, P., and S.-W. Son (2015), Onset of Circulation Anomalies during Stratospheric Vortex Weakening Events: The Role of Planetary-Scale Waves, *Journal of Climate*, 28(18), 7347–7370, doi:10.1175/JCLI-D-14-00478.1.
- Matsuno, T. (1970), Vertical Propagation of Stationary Planetary Waves in the Winter Northern Hemisphere, *Journal of the Atmospheric Sciences*, 27(6), 871–883, doi:10.1175/1520-0469(1970)027<0871:VPOSPW>2.0.CO;2.
- Matsuno, T. (1971), A Dynamical Model of the Stratospheric Sudden Warming, *Journal of the Atmospheric Sciences*, 28(8), 1479–1494, doi:10.1175/1520-0469(1971)028<1479:ADMOTS>2.0.CO;2.
- Matthewman, N. J., and J. G. Esler (2011), Stratospheric Sudden Warmings as Self-Tuning Resonances. Part I: Vortex Splitting Events, *Journal of the Atmospheric Sciences*, 68(11), 2481–2504, doi:10.1175/JAS-D-11-07.1.
- McIntyre, M. E. (1982), How well do we understand the dynamics of stratospheric warmings?, *Journal of the Meteorological Society of Japan*, 60(1), 37–65.
- Nakagawa, K. I., and K. Yamazaki (2006), What kind of stratospheric sudden warming propagates to the troposphere?, *Geophysical Research Letters*, 33(4), L04,801, doi: 10.1029/2005GL024784.

- Nishii, K., H. Nakamura, and T. Miyasaka (2009), Modulations in the planetary wave field induced by upward-propagating Rossby wave packets prior to stratospheric sudden warming events: A case-study, *Quarterly Journal of the Royal Meteorological Society*, *135*(638), 39–52, doi:10.1002/qj.359.
- Palmeiro, F. M., D. Barriopedro, R. García-Herrera, and N. Calvo (2015), Comparing Sudden Stratospheric Warming Definitions in Reanalysis Data\*, *Journal of Climate*, *28*(17), 6823–6840, doi:10.1175/JCLI-D-15-0004.1.
- Palmer, T. N. (1981), Aspects of stratospheric sudden warmings studied from a transformed Eulerian-mean viewpoint, *Journal of Geophysical Research*, *86*(C10), 9679, doi:10.1029/JC086iC10p09679.
- Polvani, L. M., and D. W. Waugh (2004), Upward Wave Activity Flux as a Precursor to Extreme Stratospheric Events and Subsequent Anomalous Surface Weather Regimes, *Journal of Climate*, *17*(18), 3548–3554, doi:10.1175/1520-0442(2004)017<3548:UWAFAA>2.0.CO;2.
- Reichler, T., and J. Kim (2008), How Well Do Coupled Models Simulate Today’s Climate?, *Bulletin of the American Meteorological Society*, *89*(3), 303–312, doi:10.1175/BAMS-89-3-303.
- Scaife, A. A., R. E. Comer, N. J. Dunstone, J. R. Knight, D. M. Smith, C. MacLachlan, N. Martin, K. A. Peterson, D. Rowlands, E. B. Carroll, S. Belcher, and J. Slingo (2017), Tropical rainfall, Rossby waves and regional winter climate predictions, *Quarterly Journal of the Royal Meteorological Society*, *143*(702), 1–11, doi:10.1002/qj.2910.
- Schneidereit, A., D. H. W. Peters, C. M. Grams, J. F. Quinting, J. H. Keller, G. Wolf, F. Teubler, M. Riemer, and O. Martius (2017), Enhanced Tropospheric Wave Forcing of Two Anticyclones in the Prephase of the January 2009 Major Stratospheric Sudden Warming Event, *Monthly Weather Review*, *145*(5), 1797–1815, doi:10.1175/MWR-D-16-0242.1.
- Schoeberl, M. R. (1978), Stratospheric warmings: Observations and theory, *Reviews of Geophysics*, *16*(4), 521–538, doi:10.1029/RG016i004p00521.
- Scott, R. K., and L. M. Polvani (2004), Stratospheric control of upward wave flux near the tropopause, *Geophysical Research Letters*, *31*(2), 1–4, doi:10.1029/2003GL017965.
- Scott, R. K., and L. M. Polvani (2006), Internal Variability of the Winter Stratosphere. Part I: Time-Independent Forcing, *Journal of the Atmospheric Sciences*, *63*(11), 2758–2776, doi:10.1175/JAS3797.1.
- Shaw, T. A., J. Perlwitz, and O. Weiner (2014), Troposphere-stratosphere coupling: Links to North Atlantic weather and climate, including their representation in CMIP5 models, *Journal of Geophysical Research: Atmospheres*, *119*(10), 5864–5880, doi:10.1002/2013JD021191.
- Sigmond, M., J. F. Scinocca, V. V. Kharin, and T. G. Shepherd (2013), Enhanced seasonal forecast skill following stratospheric sudden warmings, *Nature Geoscience*, *6*(2), 98–102, doi:10.1038/ngeo1698.
- Simpson, I. R., M. Blackburn, and J. D. Haigh (2009), The Role of Eddies in Driving the Tropospheric Response to Stratospheric Heating Perturbations, *Journal of the Atmospheric Sciences*, *66*(5), 1347–1365, doi:10.1175/2008JAS2758.1.
- Tripathi, O. P., M. Baldwin, A. Charlton-Perez, M. Charron, S. D. Eckermann, E. Gerber, R. G. Harrison, D. R. Jackson, B. M. Kim, Y. Kuroda, A. Lang, S. Mahmood, R. Mizuta, G. Roff, M. Sigmond, and S. W. Son (2015), The predictability of the extratropical stratosphere on monthly time-scales and its impact on the skill of tropospheric forecasts, *Quarterly Journal of the Royal Meteorological Society*, *141*(689), 987–1003, doi:10.1002/qj.2432.
- Tripathi, O. P., M. Baldwin, A. Charlton-Perez, M. Charron, J. C. H. Cheung, S. D. Eckermann, E. Gerber, D. R. Jackson, Y. Kuroda, A. Lang, J. McLay, R. Mizuta, C. Reynolds, G. Roff, M. Sigmond, S.-W. Son, and T. Stockdale (2016), Examining the Predictability of the Stratospheric Sudden Warming of January 2013 Using Multiple NWP Systems, *Monthly Weather Review*, *144*(5), 1935–1960, doi:10.1175/MWR-D-15-0010.1.